2018-12

FoxN1-dependent thymic epithelial cells promote T-cell leukemia development

Ghezzo, MN

10.1093/carcin/bgy127
Carcinogenesis
Oxford University Press (OUP)

FoxN1-dependent thymic epithelial cells promote T-cell leukemia development

Marinella N. Ghezzo[1,2], Mónica T. Fernandes[1,2,†], Ivette Pacheco-Leyva[3,4,†], Pedro M. Rodrigues[3,5], Rui S. Machado[1,6], Marta A.S. Araújo[3,4], Ravi K. Kalathur[1], Matthias E. Futschik[1,7,8], Nuno L. Alves[3,5], Nuno R. dos Santos[1,3,4]*

[1]Centre for Biomedical Research (CBMR), University of Algarve, 8005-139 Faro, Portugal

[2]PhD Program in Biomedical Sciences, Department of Biomedical Sciences and Medicine, University of Algarve, 8005-139 Faro, Portugal

[3]Instituto de Investigação e Inovação em Saúde (i3S), University of Porto, 4200 Porto, Portugal

[4]Institute of Pathology and Molecular Immunology of the University of Porto (IPATIMUP), 4200 Porto, Portugal

[5]Thymus Development and Function Laboratory, Instituto de Biologia Molecular e Celular, Porto, Portugal

[6]ProRegeM PhD Program, Department of Biomedical Sciences and Medicine, University of Algarve, 8005-139 Faro, Portugal

[7]Centre of Marine Sciences (CCMAR), University of Algarve, 8005-139 Faro, Portugal

[8]School of Biomedical and Healthcare Sciences, Plymouth University Peninsula Schools of Medicine and Dentistry, Plymouth, Devon, United Kingdom.

[†]These authors contributed equally to this work.

* To whom correspondence should be addressed. Nuno R. dos Santos, Instituto de Investigação e Inovação em Saúde (i3S), Rua Alfredo Allen, 208, 4200-135 Porto, Portugal, Tel: +351 220 408 800 (ext.6180); Email: nunos@ipatimup.pt

Running title: FoxN1-dependent TECs promote T-cell leukemia

Abstract

T-cell acute lymphoblastic leukemia (T-ALL) and lymphoblastic lymphomas (T-LBL) are aggressive malignancies of thymocytes. The role of thymic microenvironmental cells and stromal factors in thymocyte malignant transformation and T-ALL development remains little explored. Here, using the TEL-JAK2 transgenic (TJ2-Tg) mouse model of T-ALL/LBL, which is driven by constitutive JAK/STAT signaling and characterized by the acquisition of *Notch1* mutations, we sought to identify stromal cell alterations associated with thymic leukemogenesis. Immunofluorescence analyses showed that thymic lymphomas presented epithelial areas characterized by keratin 5 and keratin 8 expression, adjacently to epithelial-free areas negative for keratin expression. Both areas contained abundant laminin (extracellular matrix) and ER-TR7^{+} (fibroblasts) CD31^{+} (endothelial) and CD11c^{+} (dendritic) cells. Besides keratin 5, keratin-positive areas harbored medullary thymic epithelial cells (TEC) labeled by *Ulex Europaeus* agglutinin-1. By performing flow cytometry and RNA sequencing analyses of thymic lymphomas, we observed an enrichment in medullary TEC markers in detriment of cortical TEC markers. To assess whether TECs are important for T-ALL/LBL development, we generated TJ2-Tg mice heterozygous for the FoxN1 transcription factor *nude* null mutation (*Foxn1*$^{+/nu}$). Strikingly, in TJ2-Tg;*Foxn1*$^{+/nu}$ compound mice both emergence of malignant cells in pre-leukemic thymi and overt T-ALL onset were significantly delayed. Moreover, in transplantation assays leukemic cell expansion within the thymus of recipient *Foxn1*$^{+/nu}$ mice was reduced as compared to control littermates. Since thymopoesis is largely normal in *Foxn1*$^{+/nu}$ mice, these results indicate that FoxN1 haploinsufficiency in TECs has a more profound impact in thymic leukemogenesis.

Summary

Thymic epithelial cell composition is aberrant in mouse thymic lymphomas and reduced dosage of FoxN1, a chief thymic epithelial cell transcription factor, led to delayed leukemogenesis

Introduction

T-cell acute lymphoblastic leukemia (T-ALL) and T lymphoblastic lymphomas (T-LBL) are aggressive thymocyte malignancies, as supported by similarities in the immunophenotypic, genotypic and transcriptomic profile of these leukemic cells and specific stages of intrathymic T-cell differentiation (1-3). During intrathymic thymocyte differentiation, transformation events can lead to aberrant expression of oncogenic transcription factors that induce maturation arrest (4). Genetic abnormalities in T-ALL, including chromosomal translocations, point mutations, and deletions (4), typically result in the activation of signaling pathways frequently involved in cancer, most notably the PTEN/PI3K/AKT, Ras/MAPK and JAK/STAT pathways (5). Furthermore, one of the most common genetic alterations in T-ALL and T-LBL are *NOTCH1*-activating point mutations, present in more than 60% of cases (4,6). The same signaling pathways that are activated by intrinsic oncogenic mutations can also be activated by extrinsic signals provided by stromal cells in organs where T-ALL cells thrive. For example, despite the frequent presence of *Notch1* mutations, T-ALL cells were shown to respond to and be maintained *in vitro* by NOTCH ligands, such as Delta-like ligand 1 and 4 (7-9).

Several extrinsic factors promoting T-ALL growth *in vitro* and *in vivo* were identified, including interleukin (IL)-7 (10-12), IL-18 (13), insulin-like growth factor (IGF)-1 (14), ICAM-1(15) and CXCL12 (16,17). However, it remained unclear to what extent T-ALL development depends on signals from its native thymic microenvironment. In this regard, pioneering thymectomy experiments in mouse models have since long hinted that the thymic microenvironment was essential for T-cell acute leukemia/lymphoma (18,19). Subsequent reports indicated that stromal signals are important for leukemia maintenance, as the physical contact with thymic microenvironmental cells was shown to improve survival of co-cultured thymic-derived rodent primary leukemic T cells (20,21). Furthermore, histological and immunophenotypical studies showed that the thymic stroma undergoes profound alterations throughout thymic leukemogenesis in mice (22-24). Supportive of the role of the thymic microenvironment in human T-cell leukemogenesis, several T-ALL and T-LBL patients present thymic enlargement at diagnosis (3,25,26). Moreover, patient cells were shown to expand in alymphoid fetal thymic organ cultures from NOD/SCID mouse without supplementation of exogenous factors (27).

Thymopoiesis arises from incoming bone marrow progenitors that undergo T-cell differentiation upon stimulation by thymic microenvironmental molecular signals. T-cell progenitors become

committed to the cell lineage at an immature phase characterized by the occurrence of genetic rearrangements of T-cell receptor (TCR) loci and identified by variable surface expression of CD25 and CD44 proteins and absence of CD4 and CD8 expression (double negative or DN stage). Cells undergoing successful TCR β chain rearrangement express first CD8, and become immature single-positive CD8 and then also CD4 and become so-called double-positive (DP) thymocytes. Depending on successful TCR α chain generation and negative and positive selection mediated by interactions with major histocompatibility complexes (MHC), thymocytes further differentiated into mature CD4 or CD8 single-positive (SP) T cells or regulatory T cells. Thymocyte development is achieved through a well-orchestrated bidirectional communication (so-called thymic crosstalk) between stromal cells and maturing thymocytes. These interactions trigger molecular changes in the thymic stromal microenvironment that are essential for thymocyte migration, differentiation and selection of functional mature T cells tolerant to self-antigens (28). The thymic microenvironment is composed of epithelial, mesenchymal, endothelial and hematopoietic cells (B lymphocytes, dendritic cells and macrophages). Thymic epithelial cells (TEC) are essential for the architecture of the embryonic and post-natal thymus, as demonstrated by genetic inactivation of the transcription factor FoxN1, an essential master regulator of TEC differentiation (29,30). The spatial organization of the thymus into compartments is associated with functionally different TEC subpopulations that are involved in the generation of successive stages of thymocyte development (31). Of note, cortical TEC (cTEC) are involved in T-cell lineage commitment and positive selection of thymocytes expressing functional T-cell receptor complexes, while medullary TEC (mTEC) are important for the generation of self-tolerant mature T cells. This function is mediated through MHC-mediated presentation of tissue-restricted self-antigens, which are essential for the negative selection of auto-reactive thymocytes and the generation of regulatory T cells (32).

The thymic molecular and cellular players involved in stromal support of thymocyte leukemogenesis have only recently began to be explored. Our group has reported that stromal cell inactivation of the RelB transcription factor and the TNF receptor superfamily member lymphotoxin-β receptor (LTβR), both components of the noncanonical NF-κB signaling pathway, delayed T-cell leukemia development in a transgenic mouse model expressing the TEL-JAK2 (also designated ETV6-JAK2) fusion protein in the lymphoid lineage (33,34). Recently, Triplett and colleagues (35) found in another T-ALL mouse model that IGF1R was highly expressed by malignant cells and that high IGF-1 secretion by tumor-

associated thymic dendritic cells (DCs) favored leukemic cell survival. Together, these data suggest that thymic microenvironmental cells participate in the development of T-cell leukemia.

In the present study, we characterized the stromal cellular alterations in thymic leukemogenesis and found an increase in mTEC, but not cTEC molecular markers. More importantly, we found that haploinsufficiency of the *Foxn1* gene delayed thymic leukemogenesis.

Materials and methods

Mice

Mice were bred and maintained at the CBMR/UAlg and IBMC/i3S barrier animal facilities (HEPA filtration of incoming air, differential pressure, and disinfection or sterilization of room equipment and supplies), under 12 h light/dark cycles, and with autoclaved food (4RF25 diet; Mucedola, Settimo Milanese, Italy) and water *ad libitum*. Microorganism screening (Charles River, L'Arbresle, France and Idexx Bioresearch, Ludwigsburg, Germany) detected opportunistic pathogens (*Helicobacter* spp., *Pasteurella pneumotropica* and murine norovirus) in the CBMR/UAlg and IBMC/i3S experimental rooms. The animal facilities and project were approved by the i3S ethics committee and Portuguese authorities (*Direção-Geral de Agricultura e Veterinária*). All experimental procedures were performed in accordance with European (Directive 2010/63/UE) and Portuguese (*Decreto-Lei* nº113/2013) legislation. EμSRα-TEL-JAK2 (B6.Cg-Tg(Emu-ETV6/JAK2)71Ghy) transgenic mice were described before (34,36). *Foxn1*$^{+/nu}$ (B6.Cg-*Foxn1*^{nu}/J) mice, which carry the *nude* (*nu*) null allele, were obtained from *Instituto Gulbenkian de Ciência* (Oeiras, Portugal). Upon breeding the two strains, always on the C57BL/6 genetic background, we obtained TJ2-Tg;*Foxn1*$^{+/nu}$ but no viable TJ2-Tg *nu*/*nu* mice. *Foxn1*$^{+/nu}$ mice were PCR genotyped using primers 5'-GGC CCA GCA GGC AGC CCA AG and 5'-AGG GAT CTC CTC AAA GGC TTC CAG, followed by *Bsa*JI PCR product digestion. For transplantation experiments, thymic-derived leukemic cells were prepared from diseased TJ2-Tg mice, suspended in phosphate-buffered saline (PBS) solution and injected into the tail vein of non-anesthetized 8 to 12 week-old wild-type (WT) C57BL/6 mice or into 6 to 9 week-old *Foxn1*$^{+/+}$ and *Foxn1*$^{+/nu}$ littermate mice (4 x 10^6 cells per mouse). Mouse sex is indicated in figures. TJ2-Tg and leukemic cell recipient mice were monitored for leukemia development, and euthanized by CO_2 inhalation when manifesting signs of disease and reaching pre-defined endpoints (e.g. dyspnea, loss of activity and lymph node or abdomen enlargement).

Flow Cytometry detection of hematopoietic cells

Single-cell suspensions from lymphoid organs were prepared in PBS by tissue dissociation against a 70 μm cell strainer (BD Biosciences, San Jose, CA, USA). Cells were collected by centrifugation and resuspended in staining buffer (PBS with 10% fetal bovine serum [FBS; PAA Laboratories, Linz,

Austria] and 10 mM NaN_3) with fluorochrome-labeled antibodies. After washing with staining buffer, cells were analyzed in a FACS Calibur or C6 Accuri flow cytometer (BD Biosciences). Fluorescein isothiocyanate (FITC)-, R-phycoerythrin (PE)-, PE-cyanine 5 (PE-Cy5)-, or Allophycocyanin (APC)-conjugated antibodies specific for CD90.2 (30-H12), CD11c (N418), SIRPα (P84), CD3ε (145-2C11), CD24 (M1/69), CD25 (PC61), CD4 (GK1.5), CD8 (53-6.7), and CD44 (IM7; BioLegend, San Diego, CA, USA) were used. Propidium iodide (P4170, Sigma-Aldrich, St. Louis, MO, USA) staining was used to gate viable cells for analysis. Analyses were performed on CellQuest (BD Biosciences) and FlowJo (FlowJo LLC, Ashland, OR, USA) software.

Flow Cytometry detection of enzymatically dissociated thymic stromal cells

Thymic stromal cells were isolated by enzymatic digestion as previously described (37). TECs were further enriched using a MACS-based CD45+ cell depletion kit (Miltenyi Biotec, Bergisch Gladbach, Germany). Before staining, cells were treated with Fc block (anti-CD16/CD32 antibodies TruStain FcX; Biolegend). Cell suspensions were stained as described (38) with PE-conjugated anti-CD80 (16-10A1) and anti-Ly51 (6C3), PerCP-Cy5.5-conjugated anti-CD45.2 (104), APC/eFluor660-conjugated anti-CD80 (16-10A1), APC-eFluor780-conjugated anti-I-A/I-E (M5/114-15-2), eFluor660-conjugated anti-CD11c (N418), eFluor450-conjugated anti-EpCAM (G8.8) (eBioscience, San Diego, CA), and BV785-conjugated anti-Sca-1 (D7) (Biolegend). The binding of biotinylated *Ulex europaeus* agglutinin-1 (UEA-1) (Vector Laboratories, Burlingame, CA) or anti-Ly51 (6C3) was revealed by PE-Cy7-conjugated streptavidin (eBioscience). Intracellular staining with APC/eFluor660-conjugated anti-Aire (5H12) antibody (eBioscience) was performed according to the supplier's protocol. Flow cytometry data were acquired on a FACSCanto II and LSRFortessa, and analyzed on FlowJo software.

Immunofluorescence

Whole thymi were included and frozen in OCT compound (VWR, Radnor, PA, USA). Thymic cryosections of 6-10 µm were dried at 37ºC for 30 min before fixation with pre-cold acetone for 10 min at room temperature. Sections were re-hydrated in PBS, washed with PBSW solution (PBS with 0.1% Tween 20 [VWR]) and incubated with blocking solution (10% BSA [A9418, Sigma-Aldrich], 20% FBS in PBSW) for 1 h. Primary antibodies (Supplementary Table 1) were incubated overnight at 4ºC, washed with PBSW, followed by 1 h incubation with secondary antibodies (Supplementary Table 1) at room temperature. Slides were washed with PBS and mounted in Mowiol reagent with 0.15% DAPI

(Biotium, Fremont, CA, USA). Images were acquired with an Axio Imager Z2 fluorescence microscope (Carl Zeiss, Jena, Germany). Images were processed using open-source ImageJ and AxioVision (Carl Zeiss) software. Assembly of sequential images was performed using Pairwise Stitching in Fiji software.

Quantitative RT-PCR analysis of whole and stromal cell-enriched thymic samples

Stromal cell-enriched fractions were obtained by mechanically dissociating thymic tissue through a 70 µm cell strainer in PBS and collecting the tissue retained in the mesh. Total RNA from whole thymus and stromal cell-enriched thymic samples was prepared using Trizol reagent (Life Technologies, Carlsbad, CA, USA) and phenol:chloroform extraction, according to the manufacturer's instructions. Genomic DNA was removed from RNA samples with DNase I treatment (Thermo Fisher Scientific, Waltham, MA, USA). Reverse transcription was performed using the First Strand cDNA Synthesis Kit (Thermo Fisher Scientific) and oligo(dT)$_{18}$ primers, according to the manufacturer's instructions. For quantitative PCR, 2 µL of 1/20 diluted cDNA, SsoFast EvaGreen Supermix (Bio-Rad) and 300 nM of primers (Supplementary Table 2) in 20 µL were analyzed on a CFX 96 Real-time PCR detection system (Bio-Rad). The mean fold change in expression of the gene of interest was calculated in relation to expression of a reference gene (*Hprt*) by the comparative C_T method ($2^{-\Delta\Delta C(T)}$ method).

Genomic DNA extraction and Notch1 *mutation detection*

Genomic DNA was extracted from TJ2-Tg leukemic cells using the GeneJET Genomic DNA purification kit (Thermo Fisher Scientific), following the manufacturer's protocol. The exon 34 of *Notch1* was PCR amplified as previously described (39), and purified PCR products were Sanger sequenced at GenCore/i3S and CCMAR (Faro, Portugal).

Next Generation Sequencing

Thymic stromal cell-enriched fractions from WT (5 male) and TJ2-Tg (1 female and 2 male) mice were obtained as described above and total RNA was extracted using the Direct-zol RNA Miniprep kit (Zymo Research). Next, mRNA was isolated using the NEBNext Poly(A) mRNA Magnetic Isolation Module (New England Biolabs, Ipswich, MA, USA), following the manufacturer's instructions. The WT and TJ2-Tg mRNA samples were pooled and purified using the RNeasy MinElute Cleanup kit (Qiagen) and further processed using the Ion Total RNA-Seq kit v2 (Thermo Fisher Scientific).

Sequencing was performed on Ion Torrent PGM (Thermo Fisher Scientific) using Ion 316 Chip kits v2 (Thermo Fisher Scientific) for the WT and TJ2-Tg pooled samples. Both FastQC and Prinseq indicated high sequence quality except for a residual adapter sequence in a subpopulation of reads. The latter was removed by Cutadapt software. Additionally, reads were trimmed when the corresponding Phred score fell below 25. Subsequently, reads were aligned to the full mouse genome (UCSC, version mm10) by the Torrent Mapping Alignment Program (TMAP). In total, 3,204,955 WT and 3,125,039 TJ2-Tg reads were mapped to the mouse genome. Gene expression levels were obtained by HTseq-count, and differential gene expression was assessed with Bioconductor package edgeR.

Statistical analysis

Graphs and statistical analyses were performed with GraphPad Prism software (La Jolla CA, USA). Statistical tests are indicated in the figure legends. Two-tailed *t*-tests were used to determine how significant were the differences between the means of two independent samples. Welch's correction was applied when variances were unequal, as determined by the *F*-test.

Results

TEL-JAK2 transgenic mouse thymic lymphomas present profound histological changes as compared to healthy thymi

Transgenic expression of the TEL-JAK2 fusion protein in the lymphoid cell lineage (driven by the EμSRα enhancer/promoter) results in T-cell leukemia and lymphoma, affecting the thymus, spleen, lymph nodes and other organs (39). Signs of disease (labored breathing or abdominal or nodal enlargement) in EμSRα-TEL-JAK2 transgenic (TJ2-Tg) mice manifest at variable ages, usually between 8 and 20 weeks. No abnormalities in T-cell development are apparent in the initial weeks of life, but blind analysis of seemingly healthy 8-week-old TJ2-Tg mice revealed that in a subset of mice leukemic cells (identified by aberrant CD8 and CD25 co-expression) could be detected only in the thymus or in higher numbers in this organ than in other body locations (35). Further indicating that malignancy arises in the thymus, genetic blockade of T-cell development at the DP stage did not hamper leukemia/lymphoma development (40). Thymic lymphomas from TJ2-Tg mice often become 10-20 times larger than age-matched control thymi and lose the typical thymic compartmentalization in cortex and medulla (36). To characterize in more detail the thymic microenvironmental changes during TJ2-Tg-induced leukemogenesis, we assessed the spatial distribution of several thymic stromal cells in diseased mice. Immunofluorescence analysis of large thymic lymphomas from overtly ill mice with antibodies against the keratin (Krt) 5 and Krt8 epithelial cell markers revealed large cellular regions lacking both Krt5- and Krt8-labeling, here designated as keratin-negative areas (KNA) (Supplementary Figure 1A and B). In contrast to the WT thymus, where medullary (Krt5-positive) and cortical (Krt8-positive, Krt5-negative) regions were clearly spatially segregated (Figure 1, panels a1 and a2), keratin-positive areas in thymic lymphomas displayed intermingled or overlapping Krt5 and Krt8 expression (Figure 1, panels a3 and a4, and Supplementary Figure 1C). Further spatial characterization based on *Ulex Europaeus* agglutinin-1 (UEA-1) binding and DEC205 protein expression, which respectively identify mTECs and cTECs (Figure 1, panels b1-b2, and c1-c2), showed that UEA-1^{+} mTECs were found within Krt5^{+} lymphoma areas (Figure 1, panels b3 and b4).. TJ2-Tg2 thymic lymphomas displayed a dense DEC205 staining in keratin-positive regions, notably stronger in areas with weaker Krt5 staining, suggesting that DEC205 labels residual cortical areas marked by ectopic Krt5 expression (Figure 1, panels c3 and c4). Since DEC205 (encoded by the *Ly75* gene) is known to be

expressed by thymic DCs (40), DEC205$^+$ cells in thymic lymphoma KNAs (Figure 1, panel c3 and c4), could indicate the presence of DCs. Indeed, CD11c immunolabeling, a more specific DC marker, showed increased proportions of DCs in thymic lymphomas distributed both within Krt5-positive and -negative areas (Supplementary Figure 2).

As reported, fibroblast labeling by the ER-TR7 antibody was not restricted to any particular region of the WT thymus, but was more abundant in the thymic capsule, trabeculae, and lining of blood vessels (Figure 1, panels d1 and d2) (41). In TJ2-Tg thymic lymphomas, the pattern of ER-TR7 expression was similar in both keratin-positive and -negative areas, although a layer of ER-TR7$^+$ cells marked the border between these two areas (Figure 1, panels d3 and d4, and Supplementary Figure 3A). Laminin labeling was similar to ER-TR7 labeling, in that it was present throughout the tumor tissue, irrespective of keratin labeling, and marking the boundary between keratin-positive and -negative areas (Figure 1, panels e3 and e4). The CD31 marker, labeling endothelial cells, was also present throughout the thymic lymphoma tissue (Figure 1, panels f3 and f4). Double immunofluorescence analyses showed that all CD31$^+$ lymphoma blood vessels were surrounded by laminin (Supplementary Figure 3B), which is normally a component of vascular basement membranes (42).

While F4/80$^+$ macrophages were scattered in normal thymic tissue (Figure 1, panels g1 and g2), these cells were also distributed throughout thymic lymphomas, albeit more abundantly in keratin-positive areas (Figure 1, panels g3 and g4). Finally, we also analyzed the distribution pattern of the integrin-binding ICAM-1 adhesion molecule. As previously reported (43,44), ICAM-1 was detected both in the thymus cortex and medulla, although more prominently in the latter (Figure 1, panel h1). In TJ2-Tg thymic lymphomas, ICAM-1 expression was more prevalent in areas of stronger Krt5 labeling (Figure 1, panels h3 and h4), often co-localizing at the cellular level (Supplementary Figure 3C).

The immunohistological data indicate that the composition of TECs is altered in thymic lymphomas, with a predominance for mTEC marker expression. To evaluate TEC alterations through another method, we performed gene expression analysis of whole thymic lymphomas. Quantitative PCR revealed a significant decrease in Krt5 and Krt8 transcripts within lymphomas as compared to normal whole thymi, confirming the notion that the proportion of thymic epithelial cells was reduced (Supplementary Figure 4). Furthermore, the ratio of Krt5/Krt8 mRNA levels was significantly higher in lymphomas than in normal thymi (Supplementary Figure 4), thus supporting the notion that mTEC markers dominate over cTEC markers in those tumors.

Since the aforementioned results were based on analysis of large thymic lymphomas (from overtly ill TJ2-Tg mice), weighing from 500 to 1400 mg, we also assessed by immunofluorescence the extent of stromal cell alterations in smaller lymphomas, i.e. above the weight of a normal adult thymi (between 50 and 100 mg) but below 400 mg (Figure 2A). These analyses led to two main findings. First, Krt5 labeling was expanded in relation to Krt8 labeling, with concomitant loss of the normal cortico-medullary compartmentalization (Figure 2A, second row panels). Second, the extension of KNAs, which contained abundant ER-TR7^{+} fibroblasts, increased with lymphoma size (Figure 2A, third row panels). Since an evident expansion of Krt5^{+} in relation to Krt8^{+} areas was recurrently detected in TJ2-Tg thymic lymphomas, we have also immunostained thymic lymphomas for the UEA-1 medullary marker, and this led to a similar staining pattern as that of Krt5 (Figure 2A, bottom panels). These results indicate that Krt5^{+}UEA-1^{+} TECs expand in detriment of Krt8^{+} TECs during lymphoma formation.

Flow cytometry detection of thymic lymphoma-derived stromal cells

To further characterize the TEC subpopulations in TJ2-Tg thymic lymphomagenesis, we compared the representation of cTEC (defined as CD45^{-}EpCAM^{+}UEA-1^{-}Ly51^{+}) and mTEC (CD45^{-}EpCAM^{+}UEA-1^{+}Ly51^{-}) in aged-matched WT mice and TJ2-Tg mice with or without leukemic cells. Confirming the notion that cTECs decline with leukemogenesis, the proportion of cTECs was generally lower in TJ2-Tg thymic lymphomas than in WT or TJ2-Tg thymi without leukemic cells (Figure 3, compare TJ2-Tg no. 31 and 29 vs WT and TJ2-Tg no. 32). In contrast, the proportion of mTEC, including the more differentiated mTEC^{high} subpopulation (CD80^{hi}MHCII^{hi}Aire^{+}) was dominant in thymic lymphomas (Figure 3). These data indicate that thymic leukemogenesis is accompanied by loss of cTECs relative to mTECs.

Global gene expression analysis reveals alterations in thymic stromal cell composition early in leukemogenesis

To gain further insights into the nature of the stromal cell alterations in thymic leukemogenesis, we used an unbiased genome-wide transcriptomic approach. Because thymocytes represent the overwhelming majority of thymic cells and we aimed to obtain transcriptomic data from stromal populations, we depleted the former from thymic samples by mechanical disruption of thymic fragments, a procedure that mostly liberates hematopoietic cells. Since standard thymus enzymatic digestion protocols may lead to uneven depletion of specific stromal cell types (45,46), we extracted

RNA from non-digested stromal cell-enriched thymic fractions (see Materials and methods section). This fractionation method maintained a diverse set of stromal cells (including TECs, DCs and mesenchymal cells) and led to enrichment of thymic stromal cell genes and depletion (but not exclusion) of thymocyte-specific genes (Supplementary Figure 5). We compared WT with TJ2-Tg (8- to 10-week-old) mice with no external signs of disease but presenting incipient leukemogenesis, defined by normal sized thymi (<100 mg) and the presence of low proportions (10-22%) of $CD8^+CD25^+$ leukemic cells within the thymocyte population (not shown). Pooled RNA samples were subjected to high-throughput sequencing, and bioinformatic analyses disclosed 640 differentially expressed genes (DEGs), 199 upregulated in WT thymi (Supplementary Table 3) and 441 upregulated in TJ2-Tg thymi (Supplementary Table 4). As expected from the crude stromal fractionation, several genes differentially expressed between WT and TJ2-Tg samples most likely derive from T lineage cells (e.g., *Ptcra*, *Rag1*, *Rag2*, *Dntt*, *Themis*, etc.). Nevertheless, many up- or downregulated genes were well-characterized stromal cell markers (e.g. *Ccl25*, *Vim*, *Lepr*, *S100a4*, *Zbtb46*, *Xcl1*, etc.). To know if the identified DEGs reflect imbalanced representation of distinct thymic stromal cell proportions, we investigated whether they contained lineage-restricted genes expressed in particular thymic stromal cell subsets, as previously identified by Ki and colleagues (47). Interestingly, of 116 cTEC-specific genes, 17 were upregulated in WT compared to TJ2-Tg thymi whereas none was upregulated in TJ2-Tg compared to WT thymi (Figure 2B and C, and Supplementary Table 5). These findings confirm that cTEC markers are downregulated during lymphomagenesis. In contrast, mTEC-specific genes were not significantly enriched in either WT or TJ2-Tg samples. In addition, we observed that several genes specific of $Sirp\alpha^+$ DCs were upregulated in TJ2-Tg but not WT thymi (Figure 2B and C and Supplementary Table 5). These data indicate that thymic leukemogenesis in TJ2-Tg mice is accompanied by alterations in TEC subset proportions and an increase in DCs.

Foxn1 *haploinsufficiency delays the onset of TEL-JAK2-induced leukemia*

To assess whether TECs play a role in thymic leukemogenesis, we generated TJ2-Tg mice lacking one *Foxn1* allele, a gene shown to influence TEC development and maintenance in a dose-dependent manner (29). Mice carrying the *Foxn1 nude* mutation in heterozygosity presented normal proportions of thymocyte developmental stages (as defined by CD4, CD8, CD25 and CD44 expression), including those ranging from the $CD4^-CD8^-CD25^+CD44^-$ DN three to the $CD4^+CD8^+$ DP stages (Supplementary

Figure 6A and B), which are the main cellular targets for TJ2-Tg malignant transformation (48). It was reported that *Foxn1*$^{+/nu}$ mice younger than five weeks of age present lower thymic weight than WT controls (29,49,50). Since TJ2-Tg leukemia arises during adulthood, i.e. between 6 and 20 weeks, we determined the thymic weight in older mice. Although 8 or 20 week-old *Foxn1*$^{+/nu}$ mice presented slightly smaller thymi than *Foxn1*$^{+/+}$ littermates (1.1-1.3-fold difference) (Supplementary Figure 6C), no statistically significant differences in thymic weight were found when considering females alone or older mice (7- to 9-months) of both sexes (Supplementary Figure 6C and D). Strikingly, comparison of *Foxn1*$^{+/+}$ and *Foxn1*$^{+/nu}$ TJ2-Tg mouse cohorts showed that the onset of leukemia was delayed in TJ2-Tg mice with *Foxn1* haploinsufficiency (Figure 4A). Survival analysis of each sex separately revealed that *Foxn1* haploinsufficiency delayed leukemia onset in both settings (Figure 4B). Despite the different survival rates of the two cohorts, no significant differences were observed regarding end-stage tumor load (Figure 4C). Moreover, overtly diseased TJ2-Tg;*Foxn1*$^{+/nu}$ mice presented leukemic cells expressing characteristic markers (CD3, CD4, CD8, CD24 and CD25) and thymic lymphomas displayed KNAs and areas of overlapping Krt5 and Krt8 staining as control *Foxn1*$^{+/+}$ lymphomas (Supplementary Figure 7). Like in other T-ALL mouse models, TJ2-Tg leukemic cells were found to acquire activating frameshift mutations in the PEST domain-encoding *Notch1* exon 34 (>65% incidence) (Supplementary Table 6). *Notch1* PEST domain heterozygous mutations, identified by the simultaneous detection of WT and mutated sequences (Supplementary Figure 8), occurred with similar frequency, in leukemic cells from both *Foxn1* haploinsufficient and control TJ2-Tg mice (Table 1). These mutations consisted of deletions and/or insertions, often affecting the previously reported exon 34 hotspots (codons 2361 and 2398/99) (51,52) and leading to premature stop codons and predicted loss of the C-terminal PEST domain (Table 1). Together, these data indicate that FoxN1 haploinsufficiency delayed leukemogenesis without influencing the major disease characteristics.

To investigate whether thymic defects caused by *Foxn1* haploinsufficiency impacted on the earliest detectable phases of leukemogenesis, we monitored the emergence of leukemic cells in young (8 week-old) pre-disease TJ2-Tg mice through detection of CD8^{+}CD25^{+} leukemic cells within total thymocytes, (Figure 4D). At this age, leukemic cells can be detected in TJ2-Tg thymi without significant organ enlargement (34). Indeed, thymic weight in the analyzed *Foxn1*$^{+/+}$ and *Foxn1*$^{+/nu}$ TJ2-Tg mice was not significantly different and it did not correlate with the percentage of detected CD8^{+}CD25^{+} leukemic cells (Figure 4E). However, thymi from TJ2-Tg;*Foxn1*$^{+/nu}$ mice displayed a

significantly lower percentage of $CD8^+CD25^+$ cells than TJ2-Tg;*Foxn1*$^{+/+}$ thymi (7.8-fold difference; Figure 4F). Since TJ2-Tg leukemic cells are generated intrathymically (34), $CD8^+CD25^+$ cells were barely detectable in the blood, bone marrow and spleen of mice of both *Foxn1* genotypes (Figure 4F and not shown). These findings indicate that leukemic cell emergence in the thymus is delayed when *Foxn1* gene dose is reduced in TEC. Although *Foxn1* haploinsufficiency leads to a mild decrease in thymic size, which could contribute to the observed delayed leukemogenesis, the above-presented data suggest that reduction in FoxN1 expression levels in TECs has a more marked impact on leukemogenesis than on thymocyte generation and differentiation.

The Foxn1-*dependent thymic microenvironment facilitates leukemic cell expansion*

To determine the role of the *Foxn1*-dependent microenvironment in leukemia maintenance, leukemic cells were collected from diseased TJ2-Tg mice and infused into nonconditioned syngeneic *Foxn1*$^{+/nu}$ and *Foxn1*$^{+/+}$ littermate controls (Figure 5A). When manifesting signs of disease, recipient mice were killed for macroscopic and flow cytometry analyses. Although the spleen and liver were the most invaded organs, thymi from all recipient mice became infiltrated by $CD8^+CD25^+$ leukemic cells (Figure 5B). Two independent experiments using either male or female recipients were performed and each revealed a trend towards lower tumor load in *Foxn1*$^{+/nu}$ thymi (Figure 5C). Following data normalization and pooling, we found that *Foxn1*$^{+/nu}$ mice displayed statistically significant lower thymic weight than *Foxn1*$^{+/+}$ littermates (Figure 5D). In contrast, the relative splenic and hepatic tumor load was not influenced by *Foxn1* genotype (Figure 5D). These results thus indicate that *Foxn1* expression in TECs promotes leukemic cell expansion in the thymus.

Discussion

The malignant transformation of mouse or human thymocytes is triggered by the deregulation of key cellular mechanisms due to both cell-intrinsic genetic alterations and microenvironmental stimulation (53,54). Here, using a mouse model of JAK kinase-driven and *Notch1*-mutated T-ALL, we identified several microenvironmental cellular alterations associated with thymic lymphoma development and progression. These included shifts in expression of TEC markers, with loss of cortical and increase of medullary epithelial cell markers, together with increased proportions of fibroblasts, DCs and endothelial cells. Highlighting a role for TECs, we found that reducing the genetic dose of FoxN1, an essential TEC transcription factor in TEC differentiation, delayed thymic leukemogenesis.

Diseased TJ2-Tg mice present large thymic lymphomas with loss of cortico-medullary demarcation and frequent disruption of the thymic capsule (33,36). By performing immunohistological analyses against thymic keratin proteins, we observed that TJ2-Tg mouse thymic lymphomas developed conspicuous areas without keratin expression, which were more extensive in larger lymphomas. Similar observations were reported in thymic lymphomas from other mouse models (22,35). In TJ2-Tg mice, KNAs included fibroblasts and laminin-containing extracellular matrix, suggesting that leukemic cells first invade the capsular connective tissue before expanding outwardly, thus generating lymphomatous KNAs. By studying spontaneous thymic lymphomas of different sizes, we found that the normal cortico-medullary demarcation was lost. This phenomenon was accompanied by a strong reduction in cortical (Krt8-positive, Krt5-negative) areas, which is in agreement with earlier reports of cortical atrophy and medullary expansion at pre-leukemic stages of viral-induced murine thymic lymphoma (23,24,55-57). Our data thus support the concept that upon emergence of leukemic cells in the thymus, these disseminate throughout all thymic compartments, impacting on TEC differentiation and/or distribution, before invading the thymic capsule and undergoing further expansion.

FoxN1 is a pivotal transcription factor for thymus and skin epithelial cell differentiation in rodents and humans (58). However, its role in cancer is less understood. Previous evidence indicated that FoxN1 suppresses the transition from benign to malignant keratinocyte lesions (59). Another report supporting a tumor-suppressive role for *Foxn1* showed that its haploinsufficiency accelerated thymic leukemogenesis in the endogenous retrovirus-expressing AKR murine strain (60). In contrast with these data, we found that loss of a single *Foxn1* allele hindered both the onset of spontaneous TEL-

JAK2-induced leukemia/lymphoma and the thymic expansion of leukemic cells in recipient mice. Since leukemogenesis in TJ2-Tg mice is initiated in the thymus (34,48) and TECs are the only thymic cells expressing *Foxn1*, we conclude that the delayed leukemogenesis in heterozygotes is caused by FoxN1-mediated defects in TECs. Despite the observed delay in leukemia onset, all TJ2-Tg;*Foxn1*$^{+/nu}$ mice succumbed to disease with similar pathological and molecular features as *Foxn1*$^{+/+}$ controls. These findings suggest that TJ2-Tg leukemogenesis is not profoundly altered by *Foxn1* haploinsufficiency, but that it takes longer to develop, at initiation and/or progression. The finding that pre-leukemic TJ2-Tg;*Foxn1*$^{+/nu}$ mice at 8 weeks present less CD8^{+}CD25^{+} thymic cells than TJ2-Tg;*Foxn1*$^{+/+}$ mice suggests that *Foxn1* haploinsufficiency in TECs impacts disease development very early on.

Foxn1 haploinsufficiency was shown to cause a moderate reduction in thymic weight of mice under 5 weeks of different outbred and inbred strains (29,49,50). Young adult *Foxn1*$^{+/nu}$ mice (8 and 20 weeks of age) displayed a mild reduction in thymic weight, which was less evident considering females alone or older mice, but no defects in *Foxn1*$^{+/nu}$ thymocyte maturation were apparent. Further supporting the notion that delayed leukemogenesis caused by *Foxn1* haploinsufficiency is not due to a mere decrease in thymocyte cellularity, the decrease in adult thymic weight at 8 weeks of age caused by loss of one *Foxn1* allele was much less pronounced (1.3-fold) relatively to the delay in both emergence of thymic leukemic cells at 8 weeks (7.8-fold) and leukemia-related TJ2-Tg mouse death (2.2-fold higher mortality rate at 20 weeks of age). Although a putative role for reduced thymocyte cellularity cannot be formally excluded, our data indicate that the delayed thymic leukemogenesis caused by *Foxn1* haploinsufficiency results from an as yet unidentified cellular mechanism acting specifically on leukemic cell propagation but not on thymocyte development.

Although the FoxN1-mediated mechanism fostering leukemogenesis remains unclear, it is possible that leukemic cell development is more sensitive than thymocyte development to changes in expression of specific FoxN1 target genes. In this line, we observed that *Foxn1* haploinsufficiency was associated with a mild reduction in *Ccl25* thymic expression (not shown), a well-established FoxN1 target gene (30,61) and a potential T-ALL growth factor (62). Future studies should address whether this or other FoxN1 target genes (e.g. *Dll4* and *Cxcl12*) play direct roles in thymic leukemogenesis. Alternatively, FoxN1 could impinge on leukemogenesis indirectly through changes in functional properties of TECs or other thymic microenvironmental cells. Since thymic leukemogenesis is

accompanied by a disorganization in TEC marker expression, it is possible that *Foxn1*$^{+/nu}$-associated TEC differentiation defects underlie the delayed leukemia onset in TJ2-Tg;*Foxn1*$^{+/nu}$ mice. In addition, TECs were shown to regulate both thymic vascularization (63,64) and thymic DC development, differentiation and recruitment (65-67). Whether *Foxn1* haploinsufficiency in TECs is linked to vascular or DC defects warrants further investigation.

It was previously shown that RelB and LTβR proteins, both expressed in mTEC and other thymic stromal cells, contribute to leukemogenesis (33,34). Additionally, these proteins are essential for thymic medulla development and maintenance, as shown by the impaired medullary compartment of the respective knock-out mice (68,69). The notion that RelB, LTβR and FoxN1 hinder leukemogenesis and that all are expressed in mTECs suggest that these or other medullary cell types are involved in thymic leukemogenesis.

Using a panel of thymic cell markers, we detected major organizational alterations involving several thymic stromal cell types in smaller and larger TJ2-induced lymphomas. Most notably, we observed increased expression of CD31 and ER-TR7, markers for endothelial cells and thymic fibroblasts, respectively, suggesting that angiogenesis, fibroblast proliferation and accrued ECM deposition, which are often associated with cancer (70) may favor thymic lymphomagenesis, especially at the most advanced stages. We have also found expression of markers for macrophages (F4/80) and DCs (CD11c and DEC205) in lymphomas. Macrophages have been identified in mouse thymic lymphomas (23,56,71), and recent studies indicate that lymphoma-associated macrophages stimulate T-ALL proliferation *in vitro* (72). Thus, the potential involvement of tumor-associated macrophages in T-cell leukemogenesis merits further investigation. DCs are usually associated with an anti-tumoral role via their function in adaptive immunity as tumor antigen-presenting cells (73). However, it was recently shown that DCs favored survival or proliferation of B and T leukemic cells (35,74). More specifically, Triplett et al. (35) reported that thymic lymphoma-derived DCs (most notably Sirpα-positive DCs) promoted leukemic T cell survival through IGF-1 and PDGF (platelet-derived growth factor) secretion. An increased proportion of DCs and increased expression of Sirpα^{+} DC genes was found in the stroma of TJ2-Tg thymic lymphomas, so studies determining whether DCs are involved in TJ2 leukemogenesis are warranted.

Together, our findings demonstrate that the thymic microenvironment in general and TECs specifically are crucial for the malignant transformation of thymocytes. The identification of the key

molecular signals produced by stromal cells will not only shed further light on the mechanisms underlying T-cell leukemogenesis, but may also be instrumental for the design of therapies targeting these malignancies.

Supplementary material

Supplementary Figures 1 through 8 and Supplementary Tables 1 through 6 can be found at http://carcin.oxfordjournals.org/

Funding

This work was supported by: FCT - *Fundação para a Ciência e Tecnologia* / *Ministério da Ciência, Tecnologia e Inovação* (grants PTDC/SAU-OBD/103336/2008 to N.R.d.S., UID/BIM/04773/2013 to CBMR, UID/Multi/04326/2013 to CCMAR, and POCI-01-0145-FEDER-007274 to i3S), European Regional Development Fund (ERDF) through COMPETE 2020 - Operational Program for Competitiveness and Internationalization (POCI), Portugal 2020, Norte Portugal Regional Program (NORTE 2020), under the PORTUGAL 2020 Partnership Agreement, through (ERDF), in the framework of the project NORTE-01-0145-FEDER-000029, and *Núcleo Regional Sul da Liga Portuguesa Contra o Cancro* (Terry Fox scholarship to N.R.d.S.). This study was also supported by the European Research Council (ERC) under the European Union's Horizon 2020 research and innovation program (grant agreement No 637843 - TEC_Pro) - Starting grant attribute to N.L.A. FCT provided fellowships to M.N.G. (SFRH/BD/80503/2011), M.T.F. (SFRH/BD/75137/2010), and R.K.K (SFRH/BPD/96890/2013). M.N.G. received a fellowship from *Fundação* Merck Sharpe & Dohme. N.R.d.S. has been supported by FCT Ciência 2007 and FCT Investigator (IF/00056/2012) contracts.

Acknowledgements

We thank James L. Dooley, Rolf Kemler and Dietmar Vestweber for providing antibodies and Manuel Rebelo for providing B6/*nude* mice. We would like to thank Fábio Paiva and Faiza Al-Dalali for sample collection used in sequencing analyses, Ana C. Araújo, Maurícia Vinhas, Cláudia Florindo and André Mozes for technical assistance, and José A. Belo and Gabriela A. Silva for continuous support.

Conflict of Interest Statement: None declared.

References

1. Asnafi, V., *et al.* (2003) Analysis of TCR, pT alpha, and RAG-1 in T-acute lymphoblastic leukemias improves understanding of early human T-lymphoid lineage commitment. *Blood*, **101**, 2693-2703.
2. Ferrando, A.A., *et al.* (2002) Gene expression signatures define novel oncogenic pathways in T cell acute lymphoblastic leukemia. *Cancer Cell*, **1**, 75-87.
3. Baleydier, F., *et al.* (2008) T cell receptor genotyping and HOXA/TLX1 expression define three T lymphoblastic lymphoma subsets which might affect clinical outcome. *Clin Cancer Res*, **14**, 692-700.
4. Karrman, K., *et al.* (2017) Pediatric T-cell acute lymphoblastic leukemia. *Genes Chromosomes Cancer*, **56**, 89-116.
5. Girardi, T., *et al.* (2017) The genetics and molecular biology of T-ALL. *Blood*, **129**, 1113-1123.
6. Basso, K., *et al.* (2011) T-cell lymphoblastic lymphoma shows differences and similarities with T-cell acute lymphoblastic leukemia by genomic and gene expression analyses. *Genes Chromosomes Cancer*, **50**, 1063-1075.
7. Armstrong, F., *et al.* (2009) NOTCH is a key regulator of human T-cell acute leukemia initiating cell activity. *Blood*, **113**, 1730-1740.
8. Indraccolo, S., *et al.* (2009) Cross-talk between tumor and endothelial cells involving the Notch3-Dll4 interaction marks escape from tumor dormancy. *Cancer Res*, **69**, 1314-1323.
9. Minuzzo, S., *et al.* (2015) DLL4 regulates NOTCH signaling and growth of T acute lymphoblastic leukemia cells in NOD/SCID mice. *Carcinogenesis*, **36**, 115-121.
10. Scupoli, M.T., *et al.* (2007) Interleukin 7 requirement for survival of T-cell acute lymphoblastic leukemia and human thymocytes on bone marrow stroma. *Haematologica*, **92**, 264-266.
11. Silva, A., *et al.* (2011) IL-7 contributes to the progression of human T-cell acute lymphoblastic leukemias. *Cancer Res*, **71**, 4780-4789.
12. Touw, I., *et al.* (1990) Interleukin-7 is a growth factor of precursor B and T acute lymphoblastic leukemia. *Blood*, **75**, 2097-2101.
13. Uzan, B., *et al.* (2014) Interleukin-18 produced by bone marrow-derived stromal cells supports T-cell acute leukaemia progression. *EMBO Mol Med*, **6**, 821-834.
14. Medyouf, H., *et al.* (2011) High-level IGF1R expression is required for leukemia-initiating cell activity in T-ALL and is supported by Notch signaling. *J Exp Med*, **208**, 1809-1822.
15. Winter, S.S., *et al.* (2001) Enhanced T-lineage acute lymphoblastic leukaemia cell survival on bone marrow stroma requires involvement of LFA-1 and ICAM-1. *Br J Haematol*, **115**, 862-871.
16. Passaro, D., *et al.* (2015) CXCR4 Is Required for Leukemia-Initiating Cell Activity in T Cell Acute Lymphoblastic Leukemia. *Cancer Cell*, **27**, 769-779.
17. Pitt, L.A., *et al.* (2015) CXCL12-Producing Vascular Endothelial Niches Control Acute T Cell Leukemia Maintenance. *Cancer Cell*, **27**, 755-768.
18. McEndy, D.P.B., M. C.; Furth, J. (1944) On the Role of Thymus, Spleen, and Gonads in the Development of Leukemia in a High-Leukemia Stock of Mice. *Cancer Res*, **4**, 377-383.
19. Kaplan, H.S. (1950) Influence of thymectomy, splenectomy, and gonadectomy on incidence of radiation-induced lymphoid tumors in strain C57 black mice. *J Natl Cancer Inst*, **11**, 83-90.
20. Ioachim, H., *et al.* (1964) Intrareticular Cell Multiplication of Leukemic Lymphoblasts in Thymic Tissue Cultures. *J Natl Cancer Inst*, **32**, 339-359.
21. Hiai, H., *et al.* (1981) Mouse lymphoid leukemias: symbiotic complexes of neoplastic lymphocytes and their microenvironments. *J Natl Cancer Inst*, **66**, 713-722.

22. Davey, G.M., *et al.* (1996) Characterization of the AKR thymic microenvironment and its influence on thymocyte differentiation and lymphoma development. *Leuk Res*, **20**, 853-866.
23. Metcalf, D. (1966) Histologic and transplantation studies on preleukemic thymus of the AKR mouse. *J Natl Cancer Inst*, **37**, 425-442.
24. Siegler, R., *et al.* (1963) Unilateral Histogenesis of Akr Thymic Lymphoma. *Cancer Res*, **23**, 1669-1678.
25. Kersey, J., *et al.* (1975) Evidence for origin of certain childhood acute lymphoblastic leukemias and lymphomas in thymus-derived lymphocytes. *Cancer*, **36**, 1348-1352.
26. Sen, L., *et al.* (1975) Clinical importance of lymphoblasts with T markers in childhood acute leukemia. *N Engl J Med*, **292**, 828-832.
27. Ma, F., *et al.* (2002) Growth of human T cell acute lymphoblastic leukemia lymphoblasts in NOD/SCID mouse fetal thymus organ culture. *Leukemia*, **16**, 1541-1548.
28. Takahama, Y. (2006) Journey through the thymus: stromal guides for T-cell development and selection. *Nat Rev Immunol*, **6**, 127-135.
29. Chen, L., *et al.* (2009) Foxn1 is required to maintain the postnatal thymic microenvironment in a dosage-sensitive manner. *Blood*, **113**, 567-574.
30. Cheng, L., *et al.* (2010) Postnatal tissue-specific disruption of transcription factor FoxN1 triggers acute thymic atrophy. *J Biol Chem*, **285**, 5836-5847.
31. Manley, N.R., *et al.* (2010) Transcriptional regulation of thymus organogenesis and thymic epithelial cell differentiation. *Prog Mol Biol Transl Sci*, **92**, 103-120.
32. Anderson, G., *et al.* (2012) Thymic epithelial cells: working class heroes for T cell development and repertoire selection. *Trends Immunol*, **33**, 256-263.
33. dos Santos, N.R., *et al.* (2008) RelB-Dependent Stromal Cells Promote T-Cell Leukemogenesis. *PLoS ONE*, **3**, e2555.
34. Fernandes, M.T., *et al.* (2015) Lymphotoxin-beta receptor in microenvironmental cells promotes the development of T-cell acute lymphoblastic leukaemia with cortical/mature immunophenotype. *Br J Haematol*, **171**, 736-751.
35. Triplett, T.A., *et al.* (2016) Endogenous dendritic cells from the tumor microenvironment support T-ALL growth via IGF1R activation. *Proc Natl Acad Sci U S A*, **113**, E1016-1025.
36. Carron, C., *et al.* (2000) TEL-JAK2 transgenic mice develop T-cell leukemia. *Blood*, **95**, 3891-3899.
37. Meireles, C., *et al.* (2017) Thymic crosstalk restrains the pool of cortical thymic epithelial cells with progenitor properties. *Eur J Immunol*, **47**, 958-969.
38. Ribeiro, A.R., *et al.* (2014) Intermediate expression of CCRL1 reveals novel subpopulations of medullary thymic epithelial cells that emerge in the postnatal thymus. *Eur J Immunol*, **44**, 2918-2924.
39. O'Neil, J., *et al.* (2006) Activating Notch1 mutations in mouse models of T-ALL. *Blood*, **107**, 781-785.
40. Kraal, G., *et al.* (1986) Langerhans' cells, veiled cells, and interdigitating cells in the mouse recognized by a monoclonal antibody. *J Exp Med*, **163**, 981-997.
41. Van Vliet, E., *et al.* (1986) Reticular fibroblasts in peripheral lymphoid organs identified by a monoclonal antibody. *J Histochem Cytochem*, **34**, 883-890.
42. Yousif, L.F., *et al.* (2013) Laminin isoforms in endothelial and perivascular basement membranes. *Cell Adh Migr*, **7**, 101-110.
43. Lepique, A.P., *et al.* (2003) Characterization of vascular adhesion molecules that may facilitate progenitor homing in the post-natal mouse thymus. *Clin Dev Immunol*, **10**, 27-33.
44. Ueda, Y., *et al.* (2012) Mst1 regulates integrin-dependent thymocyte trafficking and antigen recognition in the thymus. *Nat Commun*, **3**, 1098.
45. Hirakawa, M., *et al.* (2018) Fundamental parameters of the developing thymic epithelium in the mouse. *Sci Rep*, **8**, 11095.

46. Sakata, M., *et al.* (2018) Cellularity of Thymic Epithelial Cells in the Postnatal Mouse. *J Immunol*, **200**, 1382-1388.
47. Ki, S., *et al.* (2014) Global transcriptional profiling reveals distinct functions of thymic stromal subsets and age-related changes during thymic involution. *Cell Rep*, **9**, 402-415.
48. dos Santos, N.R., *et al.* (2007) Pre-TCR expression cooperates with TEL-JAK2 to transform immature thymocytes and induce T-cell leukemia. *Blood*, **109**, 3972-3981.
49. Scheiff, J.M., *et al.* (1978) The thymus of Nu/+ mice. *Anat Embryol*, **153**, 115-122.
50. Kojima, A., *et al.* (1984) NFS/N-nu/ + mice can macroscopically be distinguished from NFS/N- +/+ littermates by their thymic size and shape. *Exp Cell Biol*, **52**, 107-110.
51. Lin, Y.W., *et al.* (2006) Notch1 mutations are important for leukemic transformation in murine models of precursor-T leukemia/lymphoma. *Blood*, **107**, 2540-2543.
52. South, A.P., *et al.* (2012) The double-edged sword of Notch signaling in cancer. *Semin Cell Dev Biol*, **23**, 458-464.
53. dos Santos, N.R., *et al.* (2010) NF-kappaB in T-cell Acute Lymphoblastic Leukemia: Oncogenic Functions in Leukemic and in Microenvironmental Cells. *Cancers*, **2**, 1838-1860.
54. Passaro, D., *et al.* (2016) Microenvironmental cues for T-cell acute lymphoblastic leukemia development. *Immunol Rev*, **271**, 156-172.
55. Arnesen, K. (1958) Preleukemic and early leukemic changes in the thymus of mice; a study of the AKR/O strain. *Acta Pathol Microbiol Scand*, **43**, 350-364.
56. Dunn, T.B., *et al.* (1961) Pathogenesis of a virus-induced leukemia in mice. *J Natl Cancer Inst*, **26**, 189-221.
57. Goodman, S.B., *et al.* (1963) The Histogenesis of Gross's Viral Induced Mouse Leukemia. *Cancer Res*, **23**, 1634-1640.
58. Romano, R., *et al.* (2013) FOXN1: A Master Regulator Gene of Thymic Epithelial Development Program. *Front Immunol*, **4**, 187.
59. Mandinova, A., *et al.* (2009) A positive FGFR3/FOXN1 feedback loop underlies benign skin keratosis versus squamous cell carcinoma formation in humans. *J Clin Invest*, **119**, 3127-3137.
60. Shisa, H., *et al.* (1986) Accelerating effect of nude gene heterozygosity on spontaneous AKR thymic lymphomagenesis. *Jpn J Cancer Res*, **77**, 568-571.
61. Zuklys, S., *et al.* (2016) Foxn1 regulates key target genes essential for T cell development in postnatal thymic epithelial cells. *Nat Immunol*.
62. Mirandola, L., *et al.* (2012) Notch1 regulates chemotaxis and proliferation by controlling the CC-chemokine receptors 5 and 9 in T cell acute lymphoblastic leukaemia. *J Pathol*, **226**, 713-722.
63. Bryson, J.L., *et al.* (2013) Cell-autonomous defects in thymic epithelial cells disrupt endothelial-perivascular cell interactions in the mouse thymus. *PLoS ONE*, **8**, e65196.
64. Mori, K., *et al.* (2010) Foxn1 is essential for vascularization of the murine thymus anlage. *Cell Immunol*, **260**, 66-69.
65. Ito, H., *et al.* (2006) IL-18 produced by thymic epithelial cells induces development of dendritic cells with CD11b in the fetal thymus. *Int Immunol*, **18**, 1253-1263.
66. Lei, Y., *et al.* (2011) Aire-dependent production of XCL1 mediates medullary accumulation of thymic dendritic cells and contributes to regulatory T cell development. *J Exp Med*, **208**, 383-394.
67. Mouri, Y., *et al.* (2014) NF-kappaB-inducing kinase in thymic stroma establishes central tolerance by orchestrating cross-talk with not only thymocytes but also dendritic cells. *J Immunol*, **193**, 4356-4367.
68. Boehm, T., *et al.* (2003) Thymic medullary epithelial cell differentiation, thymocyte emigration, and the control of autoimmunity require lympho-epithelial cross talk via LTbetaR. *J Exp Med*, **198**, 757-769.
69. Burkly, L., *et al.* (1995) Expression of relB is required for the development of thymic medulla and dendritic cells. *Nature*, **373**, 531-536.

70. Kalluri, R., *et al.* (2006) Fibroblasts in cancer. *Nat Rev Cancer*, **6**, 392-401.
71. Messika, E., *et al.* (1991) Radiation leukemia virus (RadLV)-induced leukemogenesis is associated with an increased number and activity of thymic macrophages. *Int J Cancer*, **48**, 924-930.
72. Chen, S.Y., *et al.* (2015) Organ-specific microenvironment modifies diverse functional and phenotypic characteristics of leukemia-associated macrophages in mouse T cell acute lymphoblastic leukemia. *J Immunol*, **194**, 2919-2929.
73. Palucka, K., *et al.* (2012) Cancer immunotherapy via dendritic cells. *Nat Rev Cancer*, **12**, 265-277.
74. Heinig, K., *et al.* (2014) Access to follicular dendritic cells is a pivotal step in murine chronic lymphocytic leukemia B-cell activation and proliferation. *Cancer Discov*, **4**, 1448-1465.

LEGENDS TO THE FIGURES

Fig. 1. Characterization of the thymic stromal cellular alterations in advanced stage thymic lymphomas from TJ2-Tg mice. Double immunofluorescence staining of a WT thymus (panels numbered 1 and 2) and two representative TJ2-Tg thymic lymphomas (mouse nº 341, panels numbered 3 and 4, except panels b3 and b4; mouse nº 128, panels b3 and b4) out of at least three analyzed, with antibodies against the indicated markers. The higher magnification panels (numbered 2 and 4) depict a thymic region encompassing both medulla and cortex (panels a2-g2) and keratin-positive and negative boundaries (panels a4 to h4). For panels a1, b1, a3 and b3 DAPI staining (blue) is shown. Scale bars: 200 μm (panels numbered 1 and 3), 400 μm (panels numbered 2 and 4). When present, dashed-line rectangles represent the magnified area.

Fig. 2. Smaller TJ2-Tg lymphomas present thymic medullary expansion and cortical reduction. **(A)** Cryosections from TJ2-Tg thymic lymphomas of the indicated weights were immunostained for Krt5, Krt8, and UEA-1 thymic epithelial markers and the ER-TR7 fibroblast marker. Asterisks indicate KNAs; dashed-line rectangles represent area magnified in the inset panel. Scale bars: 200 μm (main panels), 100 μm (inset panels). **(B)** Venn diagrams displaying the overlap between gene sets characteristic for cortical thymic epithelial cells (cTEC), medullary thymic epithelial cells (mTEChi and mTEClo), dendritic cells (DC and DCS, negative and positive for Sirpα, respectively) and fibroblasts from the Ki et al. study (47) and upregulated genes in WT versus TJ2-Tg (T-ALL) thymic stromal fractions. (C) For each stromal cell subset, the number and percentage of genes differentially expressed between WT versus TJ2-Tg (T-ALL) thymic stromal fractions is given. *P* values determined by two-tailed Fisher's exact test.

Fig. 3. TEL-JAK2-induced thymic lymphomas present an increased proportion of medullary relative to cortical thymic epithelial cells. Flow cytometry analysis of thymocyte suspensions (most left panels) and thymic stromal cells obtained from enzymatically digested tissue (all other panels) of four representative mice, a wild-type mouse, a TJ2-Tg mouse without leukemic cells (nº32) and two TJ2-Tg mice presenting thymic leukemic cells (nº31 and 29). CD4 and CD8 staining identified normal (WT and nº32) and aberrant (nº31 and 29) thymocyte populations. Gating on $EpCAM^+$ cells, i.e. TECs, allowed identification of mTECs ($UEA\text{-}1^+$) and cTECs ($Ly51^+$). Within $UEA\text{-}1^+$, distinct levels of CD80 and MHC

class II expression represent mostly immature ($CD80^{lo}MHCII^{lo}$; $mTEC^{lo}$) and more differentiated ($CD80^{hi}MHCII^{hi}$; $mTEC^{hi}$) subsets. Specialized mature $Aire^{+}$ mTECs, detected by Aire and MHCII co-expression, were also analyzed. Values represent percentage of cells within each quadrant or region.

Fig. 4. Foxn1 haploinsufficiency delays TEL-JAK2-induced leukemogenesis. **(A)** Kaplan-Meier leukemia-free survival curves for cohorts of TJ2-Tg;*Foxn1*$^{+/+}$ and TJ2-Tg;*Foxn1*$^{+/nu}$ mice, with median survivals of 16 and 23 weeks, respectively (log-rank test, *P* value ≤ 0.0001). Hazard ratio of 2.93, with 95% CI of 1.90 to 4.51. Both groups of mice include an equal ratio (1:1.6) of females to males. **(B)** Kaplan-Meier leukemia-free survival curves for cohorts of female or male mice. The median survival of females was 15 and 23 weeks for TJ2-Tg;*Foxn1*$^{+/+}$ and TJ2-Tg;*Foxn1*$^{+/nu}$, respectively (log-rank test, *P* value ≤ 0.05), and of males was 16 and 22 weeks for TJ2- Tg;*Foxn1*$^{+/+}$ and TJ2-Tg;*Foxn1*$^{+/nu}$, respectively (log-rank test, *P* value ≤ 0.0001). **(C)** Weights of thymus, spleen, lymph nodes and liver collected from full-blown diseased TJ2-Tg;*Foxn1*$^{+/+}$ and TJ2-Tg;*Foxn1*$^{+/nu}$ mice. **(D)** Thymocyte flow cytometry analysis of three representative 8-week-old TJ2-Tg mice without external signs of disease (thymic weight of each mouse is indicated) with different proportions of aberrant CD8 SP (top panels) and $CD8^{+}CD25^{+}$ cells (bottom panels). Percentage of cells in each region is shown. **(E)** Thymic weight of 8 week-old TJ2-Tg;*Foxn1*$^{+/+}$ and TJ2-Tg;*Foxn1*$^{+/nu}$ littermate mice (top panel) and its correlation with percentage of detected $CD8^{+}CD25^{+}$ thymocytes (bottom panel). **(F)** Percentage of $CD8^{+}CD25^{+}$ leukemic cells in thymic, splenic, and blood cell suspensions from same mice as in (E). (C, E, F) Data are presented with mean ± SEM. *P* values determined by two-tailed, unpaired *t*-test with Welch's correction (**, *P* ≤ 0.01; *ns*, non-significant).

Fig. 5. *Foxn1* haploinsufficiency impairs leukemic cell expansion in recipient mouse thymi. **(A)** Transplantation experiment design. **(B)** Flow cytometry detection of $CD25^{+}$ leukemic cells in thymic cell suspensions of recipient littermate mice with the indicated genotype. Data shown is representative of one of two independent experiments performed with leukemic cells originated from two different TJ2-Tg diseased mice. **(C)** Thymic weights of recipient mice from two independent experiments, one with male and another with female recipients. **(D)** Relative organ weights from recipient mice of transplantation experiments shown in (C) pooled after normalization based on the average weight of the WT (*Foxn1*$^{+/+}$) animals in each experiment. (B-D) Data are presented with mean ± SEM; *P* value determined by two-tailed, unpaired *t*-test (*, *P* ≤ 0.05; *ns*, non-significant).

Table 1. Exon 34 *Notch1* mutations in TJ2-Tg-induced mouse leukemia samples with distinct *Foxn1* genetic backgrounds.

Samples	Sex	Death (weeks)	*Notch1* ex34	Mutated codon	Mutation
TJ2-Tg;*Foxn1*$^{+/+}$					
23	M	10	mut	2362	Ins C
24	M	13	wt	-	-
27	F	10	mut	2361	Del G, Ins CC
41	F	12	wt	-	-
73	F	13	mut	2399	Ins GGGGGGG
90	M	16	mut	2361	Del C, Ins AA
263	M	19	mut	2431	Ins A
311	F	12	mut	2377	Ins C
599	M	31	wt	-	-
613	F	28	wt	-	-
633	F	12	wt	-	-
TJ2-Tg;*Foxn1*$^{+/nu}$					
10	F	15	wt	-	-
12	F	15	mut	2361	Ins TCACGGC
17	M	25	wt	-	-
26	M	16	wt	-	-
30	F	14	mut	2361	Ins CA
33	M	18	wt	-	-
37	F	54	wt	-	-
38	F	16	wt	-	-
39	F	20	wt	-	-
45	M	13	wt	-	-
47	M	60	wt	-	-
52	M	13	wt	-	-
58	M	18	mut	2398	Del G, Ins CCCGCA
62	M	27	wt	-	-

66	M	13	mut	2361	Del G, Ins CC
72	F	8	wt	-	-
88	M	9	wt	-	-
96	F	30	wt	-	-
97	F	12	wt	-	-
140	F	13	mut	2361	Del C, ins GT
292	F	15	mut	2398	Ins TTCC
579	F	36	mut	2361	Del G, Ins CC
580	M	41	wt	-	-

M, male; F, female; mut, mutated sequence; wt, wild-type sequence

Figure 1

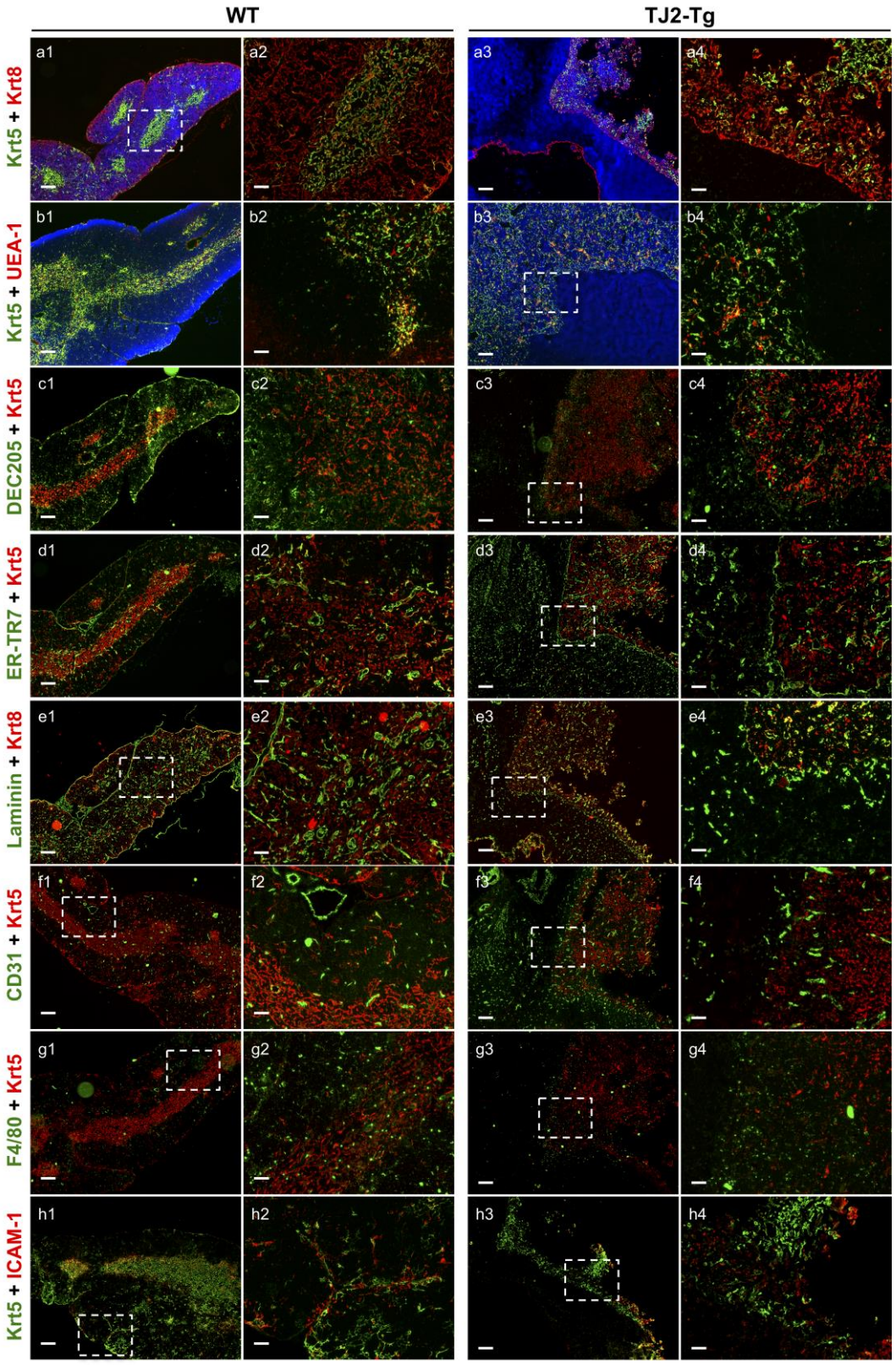

Figure 2

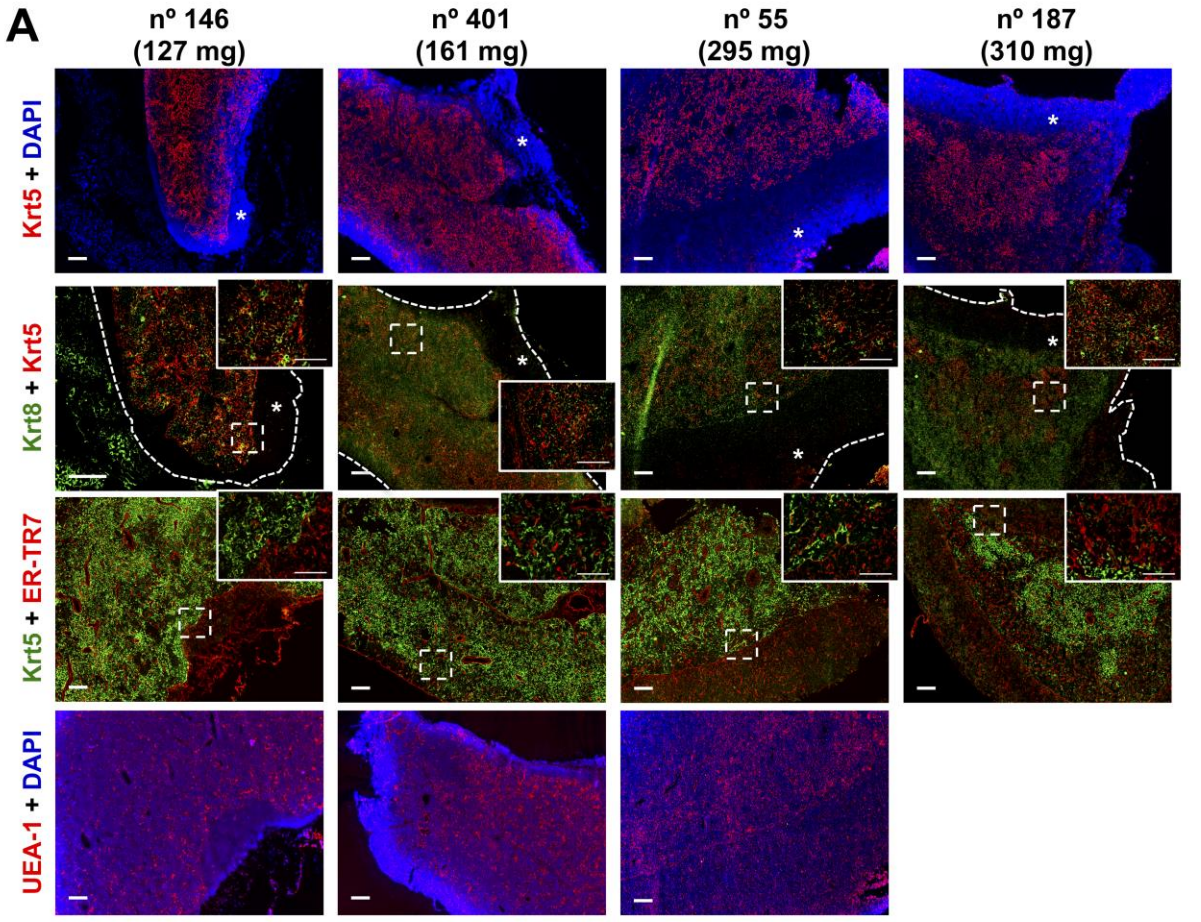

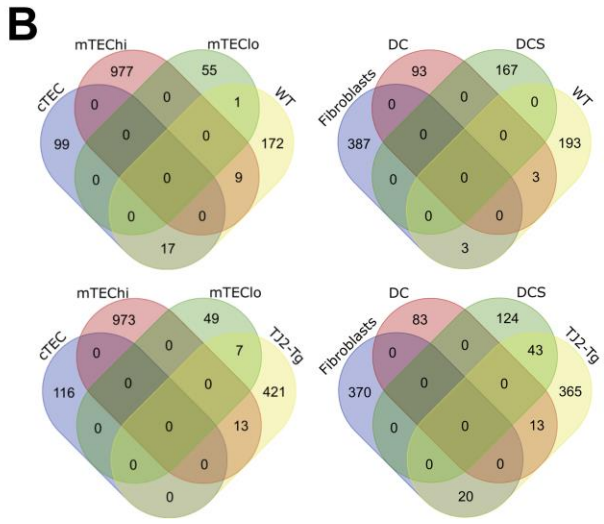

C

Stromal subsets	WT (n=199)	TJ2-Tg (n=441)	*P* value (Fisher's test)
cTEC	17 (8.5%)	0 (0.0%)	< 0.0001
mTEC^{lo}	1 (0.5%)	7 (1.5%)	0.446
mTEC^{hi}	9 (4.5%)	13 (3.0%)	0.349
Fib	3 (1.5%)	20 (4.5%)	0.066
DC	3 (1.5%)	13 (3.0%)	0.413
DCS	0 (0.0%)	43 (9.8%)	< 0.0001

Figure 3

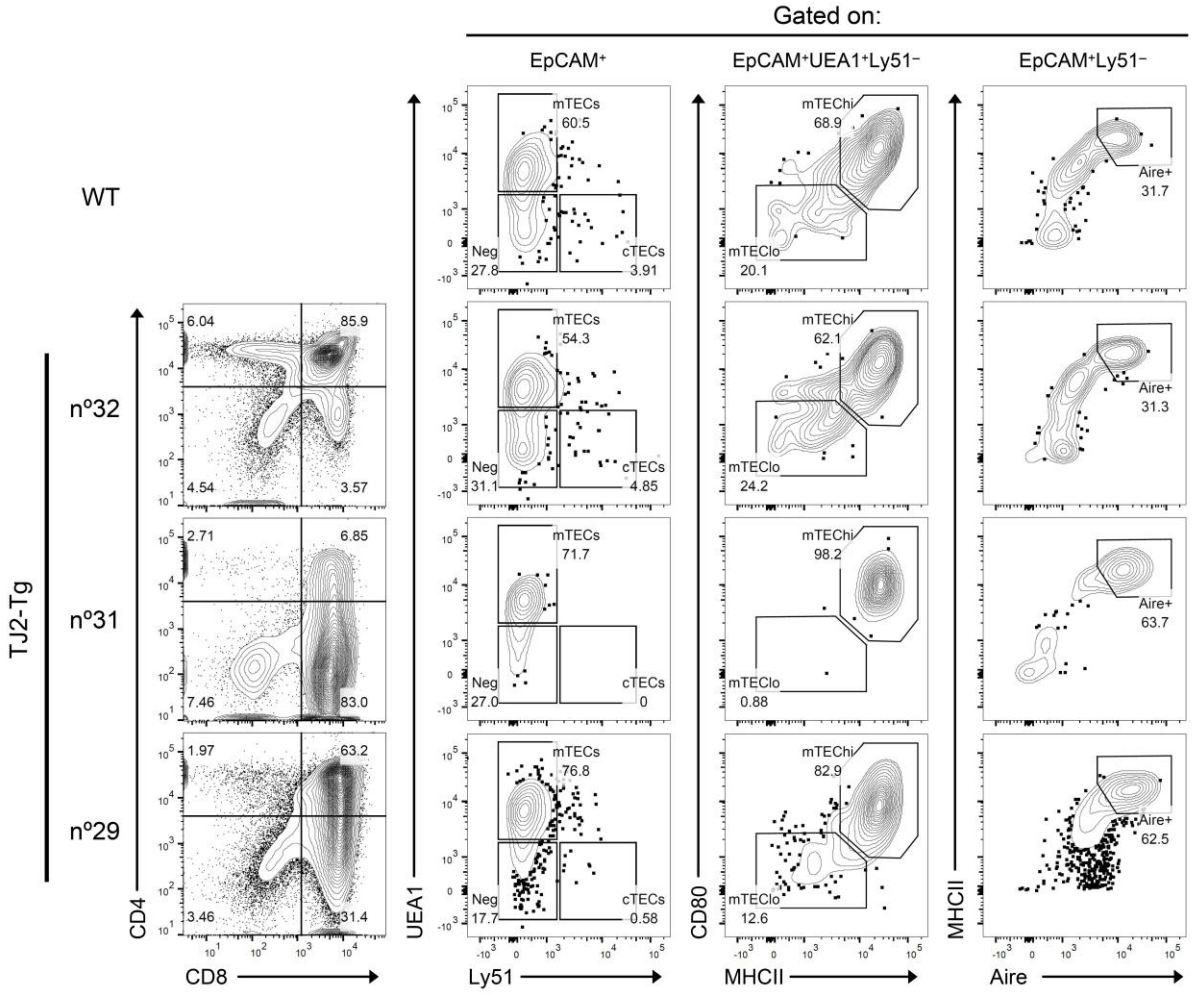

Figure 4

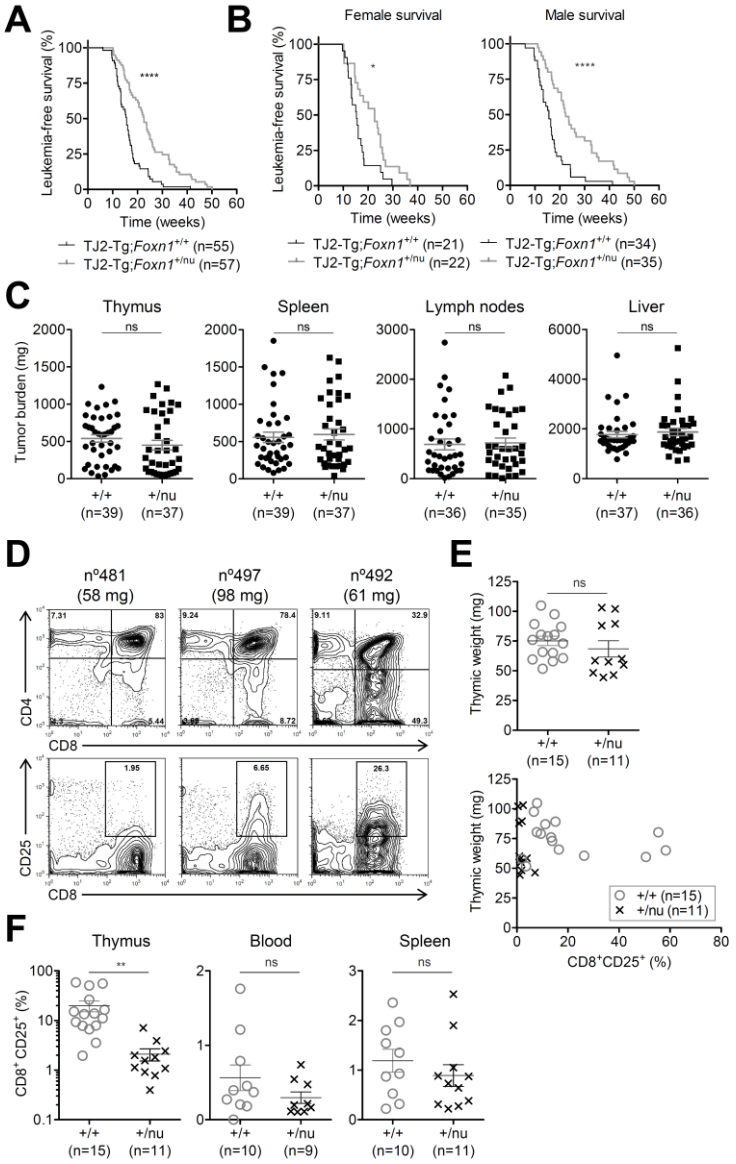

Figure 5